Inorganic Chemistry

ARTICLE

pubs.acs.org/IC

Alkynylisocyanide Gold Mesogens as Precursors of Gold Nanoparticles

Rubén Chico,[†] Eva Castillejos,[‡] Philippe Serp,[‡] Silverio Coco,*[,†] and Pablo Espinet*[,†]

[†]IU CINQUIMA/Química Inorgánica, Facultad de Ciencias, Universidad de Valladolid, 47071 Valladolid, Castilla y León, Spain

[‡]Laboratoire de Chimie de Coordination, UPR CNRS 8241 composante ENSIACET, Toulouse University, 4 Allée Monso, B. P. 44362, Toulouse Cedex 4, France

ABSTRACT: Gold nanoparticles (Au NPs) have been synthesized using simple thermolysis, whether from the mesophase or from toluene solutions, of mesogenic alkynyl−isocyanide gold complexes [Au(C≡C−C_6H_4−C_mH_{2m+1})(C≡N−C_6H_4−O−C_nH_{2n+1})]. The thermal decomposition from the mesophase is much slower than from solution and produces a more heterogeneous size distribution of the nanoparticles. Working in toluene solution, the size of nanoparticles can be modulated from ∼2 to ∼20 nm by tuning the chain lengths of the ligands present in the precursor. Different experimental conditions have been analyzed to reveal the processes governing the formation of the gold nanoparticles. Experiments on the effect of adding ligands or bubbling oxygen support that the thermal decomposition is a bimolecular process that starts by decoordination of the isocyanide ligand, producing an oxidative coupling of the akynyl group to [R−C≡C−C≡C−R] and reduction of gold(I) to gold(0) as nanoparticles. The nanoparticles obtained behave as a catalyst in the oxidation of isocyanide (CNR) to isocyanate (OCNR), which in turn cooperates to catalyze the decomposition.

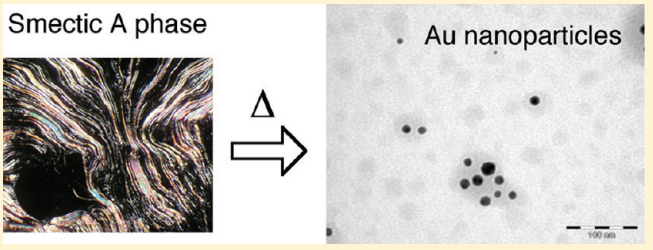

INTRODUCTION

Metal nanoparticles (MNPs) are of great interest in modern materials chemistry due to their unique physical and chemical properties.[1,2] MNPs find applications in nanoelectronics,[3] data storage,[4] catalysis,[5] and other fields. Chemical reduction, thermal decomposition, metal vapor deposition, photolysis, sonochemical decomposition, and electrochemical synthesis have been used for the synthesis of MNPs.[6] The formation of MNPs requires the presence of stabilizing ligands to control the particle size and prevent massive agglomeration.[7] To this end, stabilizers with long alkyl or polymer chains are usually employed, which attach to the MNP surface, hinder the access of the reactants to the surface and modulate the structure and properties of the MNP.

Gold nanoparticles (Au NPs) are probably the most studied ones. Recent reviews show that most often they are stabilized by organothiols. There are, however, reports on Au NPs stabilized by other ligands such as isocyanides,[8] aryl diazonium salts,[9] aryl iodoniums,[10] thiocyanates,[11] and alkynes.[12]

Two of these ligand types, alkynyls and isocyanides, happen to make a part of the rod-like gold alkynyl complexes [Au(C≡C−R)(C≡N−R′)] that have previously received attention as materials exhibiting liquid crystalline behavior[13−17] or luminescence,[18−20] as building blocks for the synthesis of nanoscale materials, or as materials for chemical vapor deposition of gold.[21,22] Very recently, we reported the synthesis and selective deposition of Au NPs inside carbon nanotubes through thermal decomposition of liquid crystalline complexes of the type [Au(C≡C−C_6H_4−C_mH_{2m+1})(C≡N−C_6H_4−O−C_nH_{2n+1})], in toluene at 110 °C. These materials are efficient catalysts for selective CO oxidation.[23] IR spectroscopy suggested that these Au NPs were stabilized by coordination of the isocyanide ligand, but no deeper studies were carried out at that moment on the mechanism of formation of the nanoparticles and the possible role of the alkynyl ligands in their stabilization.

Although the shape-controlled synthesis of Au NPs has been extensively studied,[24] its mechanism of formation has received little attention and remains partially unclear.[1c,25−27] This is particularly true in the case of Au NPs stabilized by less common ligands such as isocyanides. Therefore, we decided to study in more detail the thermal decomposition of our systems. Here, we report a facile synthesis of gold nanoparticles by thermal decomposition of mesogenic alkynylisocyanide gold complexes, either in the mesophase or in solution. On the basis of some experimental evidence, we suggest a bimolecular decomposition pathway of the initial Au(I) complexes to Au NPs.

RESULTS AND DISCUSSION

Synthesis and Characterization of Precursors. Complexes [Au(C≡C−C_6H_4−C_mH_{2m+1})(C≡N−C_6H_4−O−C_nH_{2n+1})] were prepared as air-stable white solids at room temperature, through the reaction of isocyanides with alkynylgold(I) (Scheme 1), as reported for similar systems.[14] C, H, N analyses; yields; and relevant IR and NMR data for the complexes are given in the experimental part. Their IR spectra show systematically one ν(C≡N) absorption in the range 2213−2224 cm^{-1}. As reported previously for similar systems, the expected ν(C≡C) absorption is not observed.[14] The ^{1}H NMR spectra of all of the

Received: June 6, 2011
Published: August 04, 2011

Scheme 1. Synthesis of Alkynyl−Isocyanide Gold Complexes

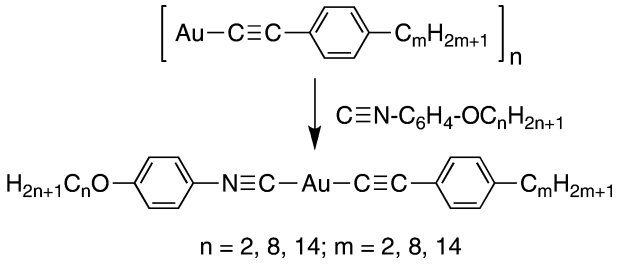

Table 1. Optical, Thermal, and Thermodynamic Data of Complexes [Au(C≡C−C$_6$H$_4$−C$_m$H$_{2m+1}$)-(C≡N−C$_6$H$_4$−O−C$_n$H$_{2n+1}$)]

			T^b	ΔH
m	*n*	transition[a]	(°C)	(kJ/mol)
2	2	C→I	183[c] (dec)	
2	8	C→C^2	91.7	12.0
		C^2→C^3	105.2	2.3
		C^3→C^4	115.6	1.3
		C^4→I	172.7 (dec)	13.2
2	14	C→C^2	25.9	4.2
		C^2→C^3	46.6	11.0
		C^3→C^4	60.2	2.0
		C^4→C^5	113.0	5.3
		C^5→SmA	140.8	15.0
		SmA→I	159[c] (dec)	*d*
8	14	C→C^2	36.4	10.2
		C^2→SmA	145.6	21.1
		SmA→I	150.2 (dec)	1.7
14	2	C→C^1	79.4	19.9
		C^1→C^2	95.1	3.0
		C^2→SmA	141.9	32.8
		SmA→I	160 (dec)	*d*
14	8	C→C^2	23.6	9.7
		C^2→C^3	81.3	4.4
		C^3→C^4	96.7	8.5
		C^4→SmA	139.9	17.4
		SmA→I	156[c] (dec)	*d*
14	14	C→C^2	41.1	1.9
		C^2→C^3	61.9	30.5
		C^3→C^4	126.9	1.4
		C^4→I	135.2	23.3

[a] C = crystal; Sm = smectic; I = isotropic liquid. [b] Data referred to the first DSC cycle. The transition temperatures are given as peak onsets. [c] Optical microscopy data. [d] Decomposition precludes measurement.

complexes are very similar and show, as expected, four resonances in the range 6.9−7.5 ppm (two AA′XX′ spin systems) for the aryl protons. In addition, the first methylene group of the alkoxy and alkyl chains is observed as a pseudotriplet (quartet for the ethoxy group) at ca. 4.0 and 2.5 ppm, respectively. The remaining hydrogen chains appear in the range 0.8−1.8 ppm.

Mesomorphic Behavior of the Precursors. The thermotropic behavior of the complexes is summarized in Table 1.

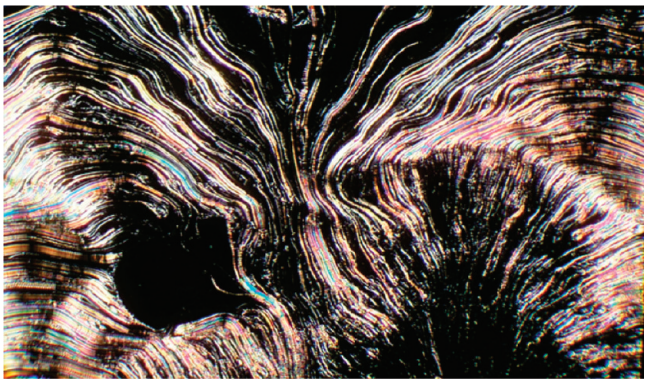

Figure 1. Polarized optical microscopic texture (×100) of the smectic A mesophase observed for [Au(C≡C−C$_6$H$_4$−C$_{14}$H$_{29}$)(C≡N−C$_6$H$_4$−O−C$_2$H$_5$)] on heating at 150 °C.

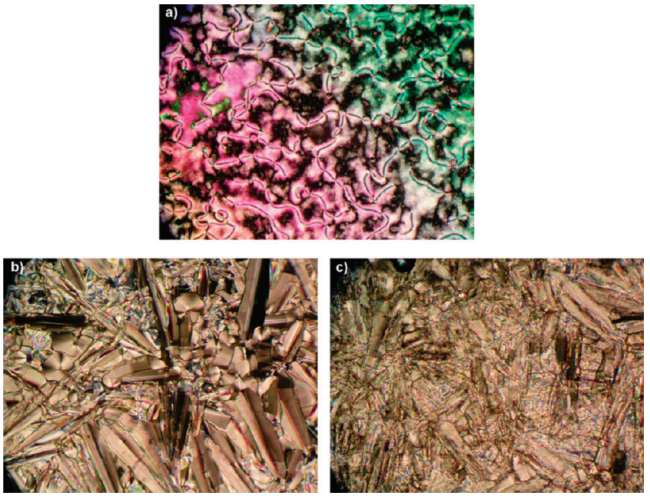

Figure 2. Polarized optical microscopic textures (×100) observed for [H$_{29}$C$_{14}$C$_6$H$_4$CC≡C−C≡CC$_6$H$_4$C$_{14}$H$_{29}$]. (a) *Schlieren* texture of the N phase, at 74 °C on cooling from the isotropic liquid. (b) Fan-shaped texture of the SmA phase at 70 °C, on cooling from the isotropic liquid. (c) Broken fan-shaped texture of the SmC phase at 58 °C formed on cooling from the fan-shaped focal-conic area of the SmA phase.

Coordination to gold enhances the intermolecular interactions, compared to the nonmesomorphic free ligands, giving rise to mesomorphic gold complexes. They display smectic A (SmA) mesophases characterized by typical homeotropic textures, reorganizing to the fan-shaped texture at temperatures close to the clearing point (Figure 1). The compounds with the shortest or the longest chains (m = 2, n = 2 and 8, and m = n = 14) are not mesomorphic. Several complexes show one or more crystal-to-crystal transitions before melting, and all of them undergo decomposition to a gold mirror upon reaching the clearing point. It is interesting to note that, at a heating rate of 10 °C min^{-1}, the decomposition temperature of the complex decreases as the total length of its two ligands (C$_m$ + C$_n$) increases.

The diacetylene with C$_{14}$, H$_{29}$C$_{14}$C$_6$H$_4$CC≡C−C≡CC$_6$H$_4$-C$_{14}$H$_{29}$, which had not been reported before, is a white solid that displays liquid crystal behavior upon heating, showing smectic C, smectic A, and nematic mesophases (see Experimental Section for details). The N mesophase displays a *Schlieren* texture

dx.doi.org/10.1021/ic201210p |*Inorg. Chem.* 2011, 50, 8654–8662

Table 2. Particle Size (Diameter in nm) of Au NPs Obtained from [Au(C≡C−C_6H_4−C_mH_{2m+1})(C≡N−C_6H_4−O−C_nH_{2n+1})] (m = 2, 8, 14; n = 2, 8, 14) after the Indicated Time at 110 °C in Toluene Solution, in the Air

entry	m	n	2 h heating	14 h heating
1	2	2	no decomposition	gold mirror
2	2	8	2.4 ± 0.1	gold mirror
3	2	14	2.2 ± 0.1	gold mirror
4	8	2	3.3 ± 0.1	gold mirror
5	14	2	7.8 ± 0.2	18.7 ± 0.5
6	14	14	8.6 ± 0.2	20.9 ± 0.4

showing singularities with two and four associated brushes (Figure 2a). The SmA mesophase was identified in optical microscopy by its focal-conic fan texture produced on cooling from the nematic mesophase (Figure 2b). The SmC mesophase shows the typical broken fan-shaped texture on cooling from the a SmA phase (Figure 2c).

Thermal Decomposition Studies. The gold complexes reported here, most of them giving rise to mesophases and to isotropic liquids at moderate temperatures, have in common with the typical stabilizers of NPs that they contain long alkyl or alkoxy chains. Thus, the generation of gold nanoparticles from these complexes in solution, in the absence of added external stabilizers, was studied. The thermolysis of the gold compounds was carried out through heating toluene solutions of [Au(C≡C−C_6H_4−C_mH_{2m+1})(C≡N−C_6H_4−O−C_nH_{2n+1})] (m = 2, 8, 14; n = 2, 8, 14) in the air at 110 °C for 2 and 14 h. The resulting solids were analyzed by TEM, and the results are collected in Table 2. It seems that the characteristics of the complexes and the nanoparticles are more influenced by the length of the alkynyl chain than by the length of the isocyanide chain: Shorter alkynyls lead to smaller nanoparticles at shorter times and produce gold mirrors at longer times; long alkynyls produce larger nanoparticles at shorter times, which grow in size at longer times but resist better the formation of gold mirrors. It is interesting to note that the rate of decomposition of the complexes under these conditions is low (as seen by IR monitoring of some of these decompositions, see later), so a high percentage of the starting complex is still unaltered after 14 h under decomposition conditions. In other words, there is a source (the starting Au(I) complex) of new Au(0) atoms available throughout the monitoring of the decomposition process.

Size and Morphology of the Au NPs. The decomposition produces predominantly spherical Au NPs, although triangular or hexagonal shapes are occasionally observed. In general, increasing the heating time from 2 to 14 h produces progressive growth in size of the nanoparticles, and eventually the formation of gold mirrors. The complexes [Au(C≡C−C_6H_4−$C_{14}H_{29}$)(C≡N−C_6H_4−O−C_nH_{2n+1})], with the longest alkynyl chain (m = 14), give more stable Au NPs, of essentially identical size for the two isocyanide chain lengths, and allow for 14 h Au NPs monitoring. Table 3 and Figure 3 show the progressive and steady increase in size of the nanoparticles with heating time.

On the other hand, TEM monitoring of [Au(C≡C−C_6H_4−$C_{14}H_{29}$)(C≡N−C_6H_4−O−C_2H_5)] after 2, 5, 8, and 14 h of heating affords histograms where the mean size of the nanoparticle increases with time, while the smaller sizes are progressively lost (Figure 4). This suggests that the growth of the nanoparticles is

Table 3. Particle Size (Diameter in nm) of Au NPs Obtained by Thermal Decomposition of [Au(C≡C−C_6H_4−$C_{14}H_{29}$)(C≡N−C_6H_4−O−C_nH_{2n+1})] in Toluene Solution, at 110°C, in the Air after Different Times

time (h)	n = 2	n = 14
2	7.8 ± 0.2	8.6 ± 0.2
5	13.6 ± 0.2	13.4 ± 0.2
8	16.6 ± 0.3	15.9 ± 0.2
14	18.7 ± 0.5	20.9 ± 0.4

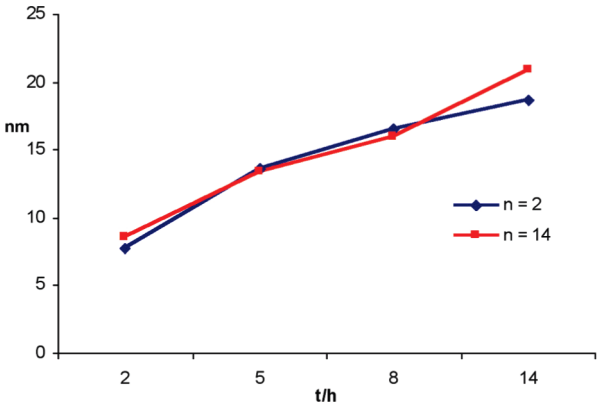

Figure 3. Nanoparticle size (diameter, nm) obtained from [Au(C≡C−C_6H_4−$C_{14}H_{29}$)(C≡N−C_6H_4−O−C_nH_{2n+1})] (n = 2, 14) as a function of heating time.

occurring not only by Ostwald ripening at the expense of redissolving the smaller particles but also by capturing the proto-nanoparticles that are continuously being formed by decomposition of the Au(I) precursor.[28,29] In other words, nucleation seems to be negligible or moderate during this growing process.

To the best of our knowledge, there is no previous report of formation of metal nanoparticles in a thermotropic mesophase that is itself generated by the molecular precursor of the metal. Thus, especially in order to check for possible morphological modifications influenced by the orientation of the molecules in the precursor phase, we studied additionally the thermal decomposition of [Au(C≡C−C_6H_4−$C_{14}H_{29}$)(C≡N−C_6H_4−O−C_2H_5)] at 155 °C for 14 h. At this temperature, the material displays a SmA mesophase. The gold nanoparticles obtained from the mesophase (Figure 5) have a smaller average diameter (12.6 ± 0.6) than those obtained from toluene solutions (18.7 ± 0.5). Moreover, they are more polydisperse and, in spite of the higher decomposition temperature used (155 °C in LC mesophase vs 110 °C in toluene solution), the rate of decomposition is smaller. It is worth noting that often the mesophases of metallomesogens are viscous, as is the case here. Clearly, the higher polydispersity of the NPs produced from the mesophase must arise from the negative effect of the high viscosity on diffusion, thus reducing the rate of Ostwald ripening. Depending on the mechanism of decomposition of the precursor molecules, the reduction of mobility caused by viscosity could also, as discussed later, cause slower decomposition rates in the mesophase compared to solution.

Studies of the Thermal Decomposition of [Au(C≡C−C_6H_4−$C_{14}H_{29}$)(C≡N−C_6H_4−O−C_2H_5)]. Gold catalyzed oxidative C−C couplings occurring in dimerizations and other organic syntheses mediated by gold complexes[30−34] are well documented to

dx.doi.org/10.1021/ic201210p |*Inorg. Chem.* 2011, 50, 8654–8662

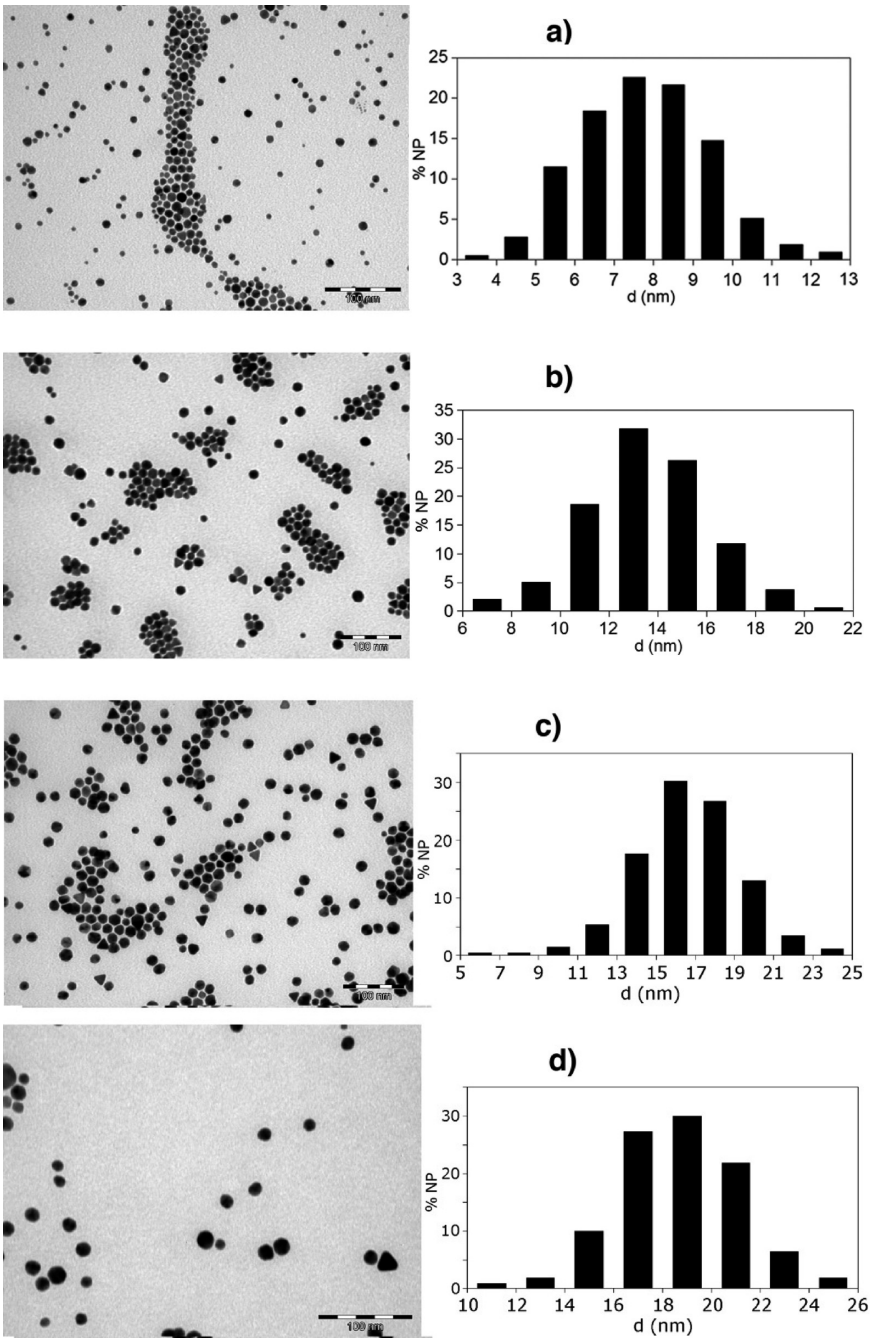

Figure 4. TEM pictures and histograms of NP size distribution obtained by thermal decomposition of $[Au(C{\equiv}C{-}C_6H_4{-}C_{14}H_{29})(C{\equiv}N{-}C_6H_4{-}O{-}C_2H_5)]$ after (a) 2, (b) 5, (c) 8, and (d) 14 h of reaction.

occur on Au(III) intermediates and require the use of strong oxidants such as Selectfluor or $PhI(OAc)_2$ in order to produce these Au(III) intermediates. Obviously, these are not the conditions under which we observe alkynyl dimerization, and a different mechanism should operate. The species clearly observed in our studies of the thermal decomposition of the alkynyl isocyanide gold(I) complexes are Au(0), either in the form of nanoparticles or as a mirror; the remaining initial isocyanide; and the dimer of the alkynyl radical, either free or coordinated to the nanoparticles (Scheme 2). The homocoupling product $[H_{29}C_{14}{-}C_6H_4{-}C{\equiv}C{-}C{\equiv}C{-}C_6H_4{-}C_{14}H_{29}]$ was identified by comparison with an independently prepared authentic sample.

To gain further insight into the process, thermal decompositions of $[Au(C{\equiv}C{-}C_6H_4{-}C_{14}H_{29})(C{\equiv}N{-}C_6H_4{-}O{-}C_2H_5)]$ in toluene solution were monitored by IR spectroscopy under different conditions (Figure 6). Interesting observations were made, which are discussed below by blocks in order to facilitate the conclusions.

1. In the absence of any additive (Figure 6, left), the color of the toluene solution changed from yellow to red as the sample was heated. Successive IR spectra of the reaction mixture in toluene show an intense $\nu(C{\equiv}N)$ absorption corresponding to the remaining gold precursor (2205 cm^{-1}), and a second $\nu(C{\equiv}N)$ absorption at 2128 cm^{-1}, progressively increasing in

dx.doi.org/10.1021/ic201210p |*Inorg. Chem.* 2011, 50, 8654–8662

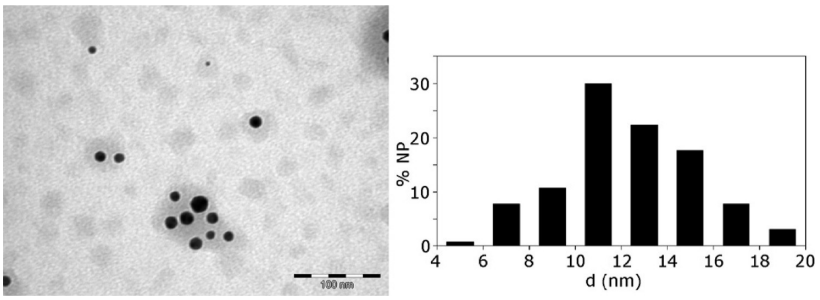

Figure 5. TEM pictures and histogram with size distribution of gold NPs obtained by decomposition of $[Au(C{\equiv}C{-}C_6H_4{-}C_{14}H_{29})(C{\equiv}N{-}C_6H_4{-}O{-}C_2H_5)]$ by heating for 14 h in the liquid crystal state at 155 °C.

Scheme 2. Stoichiometry of the Thermal Decomposition

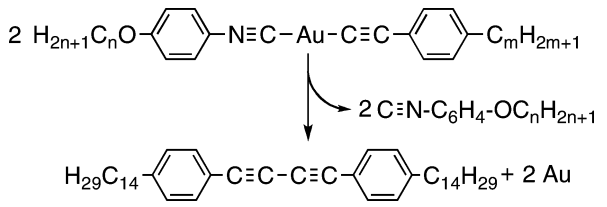

intensity, corresponding to free isocyanide. After 14 h, the IR spectrum of the nanoparticles extracted in hexane (where the gold precursor is insoluble) shows, in addition to the free isocyanide band at 2128 cm^{-1}, a weak $\nu(C{\equiv}N)$ absorption at 2195 cm^{-1} (Figure 6, left, spectrum labeled as 14 h (hexane)). This weak absorption was not observable in the toluene solution because it was overlapped by the strong absorption of the precursor at 2205 cm^{-1} and has been assigned to p-alkoxyphenyl isocyanide bonded to Au NPs.[35] These observations suggest that part of the isocyanide released upon decomposition of the precursor gold compound is involved in the stabilization of the Au NP.[8]

The IR assignments were confirmed and completed by ^1H NMR in $CDCl_3$ on samples obtained evaporating to dryness the toluene solutions and dissolving the dry residues in $CDCl_3$. The ^1H NMR spectrum of the material obtained after heating $[Au(C{\equiv}C{-}C_6H_4{-}C_{14}H_{29})(C{\equiv}N{-}C_6H_4{-}O{-}C_2H_5)]$ for 14 h confirms the presence of an unaltered gold precursor, and also the presence of the bis-alkyne homocoupling product $[H_{29}C_{14}{-}C_6H_4{-}C{\equiv}C{-}C{\equiv}C{-}C_6H_4{-}C_{14}H_{29}]$, which had not been observed in the IR spectrum.[36] This assignment was made comparing its ^1H NMR spectrum with that of an original sample of $[H_{29}C_{14}{-}C_6H_4{-}C{\equiv}C{-}C{\equiv}C{-}C_6H_4{-}C_{14}H_{29}]$, prepared independently.

Evaporation of the reactions and extraction in hexane of the dry residues extracted only the nanoparticles and the homocoupling product. So the unaltered remains of starting materials were filtered off, and evaporation of the hexane extracts afforded purified materials containing Au NPs. Again, these purified materials did not show C≡C stretching bands associated with the alkyne group in the IR spectra (neither in solution nor in the solid state), but the presence of bis-alkynes was confirmed by ^1H NMR, which also showed bands associated with isocyanide. The absence of C≡C bands has been reported to occur for alkynyl groups bonded to nanoparticles.[37,38] In this regard, DFT calculations predict a

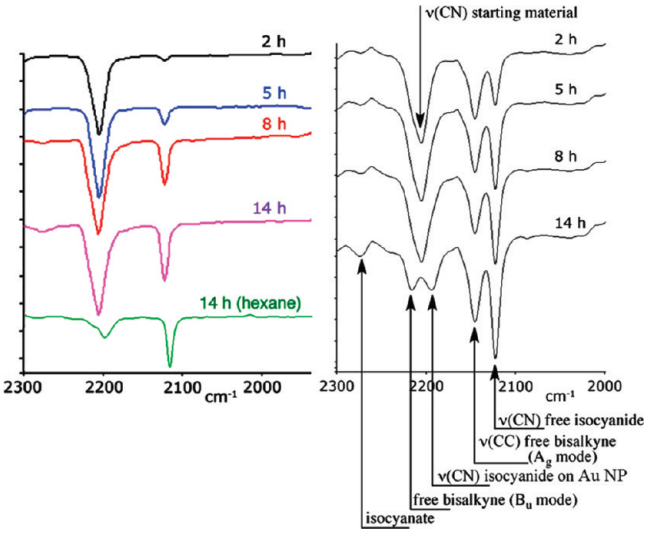

Figure 6. Left: IR monitoring of the decomposition of $[Au(C{\equiv}C{-}C_6H_4{-}C_{14}H_{29})(C{\equiv}N{-}C_6H_4{-}O{-}C_2H_5)]$ in toluene, as a function of heating time: 2, 5, 8, and 14 h. Down, in green, spectrum of a sample heated for 14 h and extracted in hexane, where the remaining precursor is insoluble. Right: IR monitoring of the decomposition of $[Au(C{\equiv}C{-}C_6H_4{-}C_{14}H_{29})(C{\equiv}N{-}C_6H_4{-}O{-}C_2H_5)]$ with $[H_{29}C_{14}{-}C_6H_4{-}C{\equiv}C{-}C{\equiv}C{-}C_6H_4{-}C_{14}H_{29}]$ as additive (1:5), dissolved in toluene, as a function of heating time (2, 5, 8, and 14 h).

bonding energy of 0.67 eV (15.45 kcal mol^{-1}) for acetylene bonded to an Au_{19} nanoparticle.[39]

2. Heating for very long times (up to 64 h) produces aggregation of the Au NPs, leading to gold mirrors. However, aggregation is not complete, and some groups of nanoparticles can still be observed (Figure 7).

After 30 h of heating, the IR spectra show small amounts of free isocyanide, the disappearance of the precursor complex, a weak $\nu(C{\equiv}N)$ absorption at 2195 cm^{-1}, which is characteristic of p-alkoxyphenyl isocyanides bonded to gold nanoparticles,[35] and a strong band at 2275 cm^{-1} (Figure 8). The appearance of this strong band at 2275 cm^{-1} as that of free isocyanide disappears suggests oxidation of the isocyanide to the corresponding isocyanate $[C_2H_5{-}O{-}C_6H_4{-}N{=}C{=}O]$, which was fully identified by mass spectroscopy [MS (CI, methane) m/z (relative intensity, %): 164 ($[M+H]^+$, 100); calcd. for $[M+H]^+$: 164.07]. Once this characteristic band had been identified, the presence of isocyanate could be noted also in Figure 6 (left), at least at the late stages of the reaction. Both the oxidation of RNC

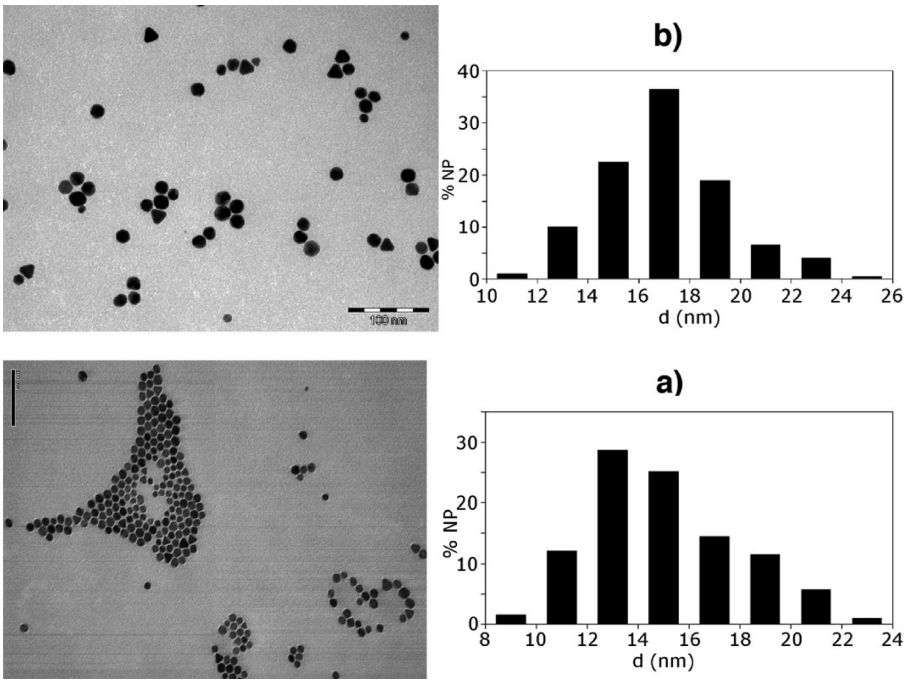

Figure 7. TEM pictures and histograms with size distribution of Au NPs obtained through thermolysis of [Au(C≡C−C_6H_4−$C_{14}H_{29}$)(C≡N−C_6H_4−O−C_2H_5)] after (a) 30 and (b) 64 h of heating.

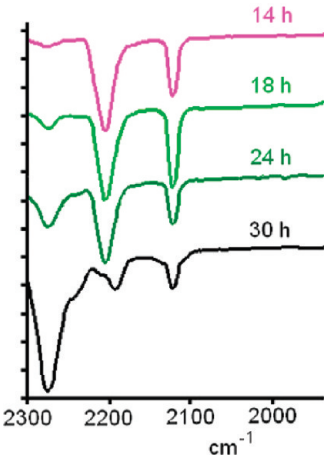

Figure 8. IR spectra (compensated toluene) of [Au(C≡C−C_6H_4−$C_{14}H_{29}$)(C≡N−C_6H_4−O−C_2H_5)] as function of heating time (14, 18, 24, and 30 h).

to RNCO and the disappearance of the starting gold(I) complex seem to occur at higher rates as the decomposition progresses. The fact that the oxidation appears to become faster at the later stages of decomposition (in contrast, the free isocyanide remains almost unaltered after refluxing for 14 h in toluene) suggests that isocyanide oxidation is favored by coordination to nanoparticles, as reported for other isocyanides bonded to metal surfaces,[40] and the consumption of isocyanide is, in turn, favoring the decomposition of the starting complex.

3. Interestingly, in a separated experiment, the thermal decomposition of [Au(C≡C−C_6H_4−$C_{14}H_{29}$)(C≡N−C_6H_4−O−C_2H_5)] in the presence of added [$H_{29}C_{14}$−C_6H_4−C≡C−C≡C−C_6H_4−$C_{14}H_{29}$] (1:5) showed a clear acceleration of the decomposition process (Figure 6, right). Thus, after 2 h of heating, the IR spectrum of the crude reaction displays three absorption bands, at 2128, 2145, and 2205 cm^{-1}, corresponding respectively to ν(C≡N) (free isocyanide), ν(C≡C) (free diacetylene), and ν(C≡N) from the remaining gold precursor. The amount of free isocyanide formed after 2 h is larger than observed in the experiment without added diacetylene; moreover, the ν(C≡N) band of the precursor is completely lost after 14 h of heating, that is, at a much faster rate than in the experiment carried out in the absence of added bis-alkyne; this allows for the additional observation of the band at 2216 cm^{-1} of the bis-alkyne and the ν(C≡N) absorption at 2195 cm^{-1} of isocyanide bonded to Au NP. An additional observation that turns out to be interesting is the appearance, already at early stages of the reaction, of the band at 2275 cm^{-1}, revealing the presence of isocyanate OCNR (see later for details).

4. In contrast, no decomposition is observed upon heating for 14 h [Au(C≡C−C_6H_4−$C_{14}H_{29}$)(C≡N−C_6H_4−O−C_2H_5)] in toluene in the presence of added [C≡N−C_6H_4−O−C_2H_5] (1:10). The fact that added [C≡N−C_6H_4−O−C_2H_5] blocks so efficiently the decomposition process suggests that ligand dissociation is required for the decomposition mechanism. Associated with this, since free isocyanide is a decomposition product, its progressive formation should have a detrimental effect on the rate of decomposition as the reaction progresses, although this may be counterbalanced by the oxidation effect discussed in entry 5.

5. When the decomposition is carried out under slow O_2 bubbling through the solution, a faster decomposition is observed, as shown in Figure 9 where a direct comparison of the ratio of the IR bands can be easily made. The band of free isocyanide at 2128 cm^{-1} is an indirect measure of decomposition, and the band for coordinated isocyanide, at 2205 cm^{-1}, measures the remaining gold precursor. It is clear that the ratio of these two

dx.doi.org/10.1021/ic201210p |*Inorg. Chem.* 2011, 50, 8654–8662

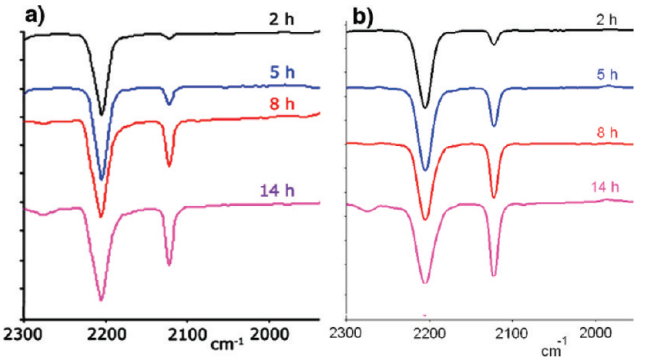

Figure 9. IR spectra for direct comparison of the rate of decomposition of $[Au(C{\equiv}C{-}C_6H_4{-}C_{14}H_{29})(C{\equiv}N{-}C_6H_4{-}O{-}C_2H_5)]$ (a) in the air and (b) under O_2 bubbling.

bands (an indirect measure of decomposed vs starting materials) increases more rapidly under O_2 bubbling (Figure 9b).

Interestingly, when the decomposition was carried out under N_2, the IR monitoring hardly showed any difference with the reaction under air. This suggests that isocyanide dissociation is the main route for decomposition, whereas isocyanide oxidation (which helps to this dissociation) is relatively inefficient and occurs only in small or catalytic amounts when O_2 bubbling is used.

The complexity and physical conditions of the system under study do not allow for a controlled quantitative kinetic study. Moreover, the main products of decomposition (bis-alkyne and isocyanide) should have opposite effects on the rate of decomposition but are at the same time involved (in unknown proportions) in the stabilization of the Au NP. Hence, a simple kinetic dependence cannot be expected. This difficulty reduces the available information to support a mechanistic proposal for the decomposition, but at least we know that the proposal should account for the qualitative observations just discussed; namely, (i) an excess of bis-alkyne induces a faster decomposition and consequently accelerates the formation of nanoparticles; (ii) an excess of isocyanide quenches the decomposition process; (iii) O_2 bubbling shows some accelerating effect.

Mechanistic Proposal for the Thermal Decomposition of [Au(C≡C−R)(C≡N−R′)] Complexes. It is well-known that C≡C bonds can π-coordinate gold. A representative example is the polymeric complex $[Au(C{\equiv}C{-}Bu^t)]_n$, where the alkynyl ligand adopts both η^1 and η^2 coordination modes.[41,42] These polymeric alkynyl complexes react with Lewis bases (L) to give a variety of [Au(C≡C−R)L] complexes. However, for ligands with hard donor atoms and lower bonding ability toward gold, the mixed alkynyl-L gold(I) complexes are often formed only in the presence of a large excess of ligand.[43] Therefore, it is not unexpected that a large excess of a relatively poorly coordinating fragment (the bis-alkyne, or the triple bond of a second molecule of the starting isocyanide−alkynylgold precursor) can promote decoordination of isocyanide from the starting gold complex, producing a faster decomposition, as observed. In this regard, it is interesting to note that the stability of π-alkyne complexes increases with increasing the electron-withdrawing character of X in [XC≡CX] alkynes.[44] Thus, the coordination strength of R−C≡C−C≡C−R through one C≡C bond should be higher than that of an isolated R−C≡C−R group. Moreover, dissociation of isocyanide in catalytic amounts could be produced by its oxidation to isocyanate, so that a C≡C bond could occupy the vacant site as a π ligand not needing to displace a strongly coordinated isocyanide ligand.

Scheme 3. Proposed Mechanism for the Thermal Decomposition of Alkynyl−Isocyanide Gold Complexes to Give Gold Nanoparticles: (i) without Addition of External Dialkynyl, (ii) Caytalyzed by Large Excess of Added Dialkynyl

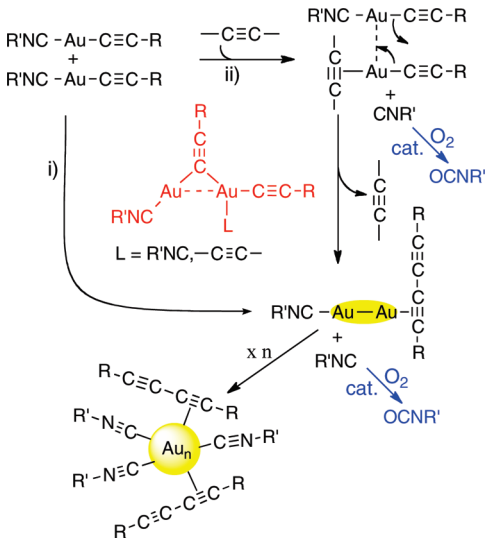

A plausible mechanism operating for the decomposition of these complexes to eventually give nanoparticles, consistent with all the observations, is depicted in Scheme 3. The decomposition patway is proposed to be bimolecular. The transmetalation intermediate (highlighted in red) leading to the confluence of the two alkynyl groups on the same atom (a prerequisite for C−C coupling to occur) involves a bridging alkynyl group, and its formation might be helped by aurophillic interactions. Alkynyl transmetalations in transition metals are very well documented.[45] From that intermediate, the coupling of the two alkynyls produces a dinuclear complex of Au(0) precariously stabilized by isocianyde and the bisalkyne, which is the protoparticle to be incorporated to others, with partial release of the stabilizing ligands.

In summary, alkynyl−isocyanide gold complexes are useful precursors of stable gold nanoparticles in the absence of added stabilizers. The decomposition can be produced from the mesophase or from solutions of these metallomesogens but is noticeably faster from solutions and produces more homogeneous particle sizes. The thermal decomposition probably starts by decoordination of an isocyanide ligand (either by itself or assisted in part by its slow oxidation to isocyanate) followed by alkynyl transmetalation from the less electrophillic to the more electrophilic gold center created upon isocyanide decoordination. This transmetalation leads to oxidative coupling of the two akynyl groups to R−C≡C−C≡C−R and reduction of gold(I) to gold(0) dimers, which eventually agglomerate into nanoparticles. The NP obtained would catalyze the oxidation of isocyanide (CNR) to isocyanate (OCNR), which explains the observed acceleration of the decomposition as the reaction progresses. The slower decomposition rates observed in the thermotropic mesophase, as compared to the solution, should be mostly due to the slower molecular diffusion in that viscous medium, which is detrimental for a bimolecular decomposition process.

dx.doi.org/10.1021/ic201210p |*Inorg. Chem.* 2011, 50, 8654–8662

EXPERIMENTAL SECTION

Combustion analyses were performed with a Perkin-Elmer 2400 microanalyzer. IR spectra were recorded on a Perkin-Elmer FT BX instrument and ^{1}H NMR spectra on Bruker AC 300 or ARX 300 instruments in $CDCl_3$. Mass spectra were recorded using an Agilent Technologies 5973 inert mass selective detector spectrometer. Microscopy studies were carried out using a Leica DMRB microscope provided with a Mettler FP82HT hot stage and a Mettler FP90 central processor, at a heating rate of 10 °C min^{-1}. For differential scanning calorimetry (DSC), a Perkin-Elmer DSC7 instrument was used, which was calibrated with water and indium; the scanning rate was 10 °C min^{-1}. The samples were sealed in aluminum capsules in the air, and the holder atmosphere was dry nitrogen. TEM observations were performed on a Hitachi HF2000 (200 kV) or a JEOL 1011 (110 kV) electron microscope. At least 200 particles were used to determine the mean diameter of the Au NP.

Literature methods were used to prepare [HC≡C−C_6H_4−C_mH_{2m+1}][46] and [C≡N−C_6H_4−O−C_nH_{2n+1}].[14] The isocyanide [C≡N−C_6H_4−O−$C_{14}H_{29}$] had not been described before, and its spectroscopic data are as follows: MP = 40.0 °C. IR (CH_2Cl_2), ν(C≡N)/cm^{-1}: 2127 (s). ^{1}H NMR ($CDCl_3$, 300 MHz): δ 0.89 (t, 3H, J = 6.6 Hz, CH_3), 1.27−1.78 (24H, alkyl chains), 3.96 (t, 2H, J = 6.6 Hz, CH_2−O), 6.86 (d, 2H, J = 8.8 Hz, H-aryl), 7.30 (d, 2H, J = 8.8 Hz, H-aryl).

All new complexes [Au(C≡C−C_6H_4−C_mH_{2m+1})(C≡N−C_6H_4−O−C_nH_{2n+1})] were prepared as reported for similar complexes.[14] A sample preparation is given: [C≡N−C_6H_4−O−C_nH_{2n+1}] (1.90 mmol) was added to [Au(C≡C−C_6H_4−C_mH_{2m+1})]$_n$ (1.27 mmol) suspended in toluene (40 mL). The resulting solution was stirred for 15 min. Then, the solvent was eliminated under reduced pressure, and a white residue was obtained. Recrystallization from CH_2Cl_2/hexane afforded white crystals of the product, 60−90% yield. Spectroscopic and analytical data are as follows:

***m* = 2, *n* = 2.** Yield: 60%. ^{1}H RMN ($CDCl_3$, 300 MHz): δ 1.21 (t, 3H, J = 7.8 Hz, CH_3, alkynyl), 1.44 (t, 3H, J = 6.3 Hz, CH_3, isocyanide), 2.62 (q, 2H, J = 7.6 Hz, C≡$CC_6H_4CH_2$), 4.07 (q, 2H, J = 7.0 Hz, C≡$NC_6H_4OCH_2$), 6.92 (d, 2H, J = 8.9 Hz, C≡NC_6H_4O−), 7.07 (d, 2H, J = 8.4 Hz, C≡CC_6H_4), 7.39 (d, 2H, J = 8.4 Hz, C≡CC_6H_4), 7.44 (2H, d, J = 8.9 Hz, C≡NC_6H_4O−). IR ν(C≡N)/cm^{-1}: 2209 (KBr), 2214 (CH_2Cl_2). Analysis calculated for $C_{19}H_{18}NOAu$ (%): C, 48.22; H, 3.83; N, 2.96. Found: C, 48.27; H, 3.89; N, 3.02.

***m* = 2, *n* = 8.** Yield: 80%. ^{1}H RMN ($CDCl_3$, 300 MHz): δ 0.89 (t, 3H, J = 7.6 Hz, CH_3, isocyanide), 1.21 (t, 3H, J = 7.7 Hz, CH_3, alkynyl), 1.30 (m, 8H, CH_2, isocyanide), 1.45 (2H, m, CH_2, isocyanide), 1.78 (m, 2H, C≡$NC_6H_4OCH_2CH_2$), 2.62 (q, 2H, J = 7.6 Hz, C≡$CC_6H_4CH_2CH_3$), 3.98 (t, 2H, J = 6.4 Hz, C≡$NC_6H_4OCH_2CH_2$), 6.93 (d, 2H, J = 9.0 Hz, C≡NC_6H_4O−), 7.08 (d, 2H, J = 8.3 Hz, C≡CC_6H_4−), 7.40 (d, 2H, J = 8.3 Hz, C≡CC_6H_4−), 7.43 (d, 2H, J = 8.9 Hz, C≡NC_6H_4O−). IR ν(C≡N)/cm^{-1}: 2210 (KBr), 2214 (CH_2Cl_2). Analysis calculated for $C_{25}H_{30}NOAu$ (%): C, 53.86; H, 5.42; N, 2.51. Found: C, 53.95; H, 5.28; N, 2.55.

***m* = 2, *n* = 14.** Yield: 79%. ^{1}H RMN ($CDCl_3$, 300 MHz): δ 0.89 (t, 3H, J = 7.0 Hz, CH_3, isocyanide), 1.22 (t, 3H, J = 7.7 Hz, CH_3, alkynyl), 1.27 (m, 20H,CH_2, isocyanide), 1.45 (m, 2H, CH_2, isocyanide), 1.81 (m, 2H, C≡$NC_6H_4OCH_2CH_2$), 2.63 (q, 2H, J = 7.7 Hz, C≡$CC_6H_4CH_2CH_3$), 3.99 (t, 2H, J = 6.4 Hz, C≡$NC_6H_4OCH_2CH_2$), 6.94 (2H, d, J = 8.9 Hz, C≡NC_6H_4O−), 7.09 (d, 2H, J = 8.0 Hz, C≡CC_6H_4), 7.41 (d, 2H, J = 8.0 Hz, C≡CC_6H_4), 7.45 (d, 2H, J = 8.9 Hz, C≡NC_6H_4O−). IR ν(C≡N)/cm^{-1}: 2211 (KBr), 2214 (CH_2Cl_2). Analysis calculated for $C_{31}H_{42}NOAu$ (%): C, 58.03; H, 6.60; N, 2.18. Found: C, 57.86; H, 6.32; N, 2.29.

***m* = 8, *n* = 14.** Yield: 82%. ^{1}H RMN ($CDCl_3$, 300 MHz): δ, 0.88 (m, 6H, CH_3), 1.26−1.58 (m, 34H, alkyl chain), 1.81 (m, 2H, C≡$NC_6H_4OCH_2CH_2$), 2.57 (t, 2H, 7.4 Hz,C≡$CC_6H_4CH_2$), 3.99 (t, 2H, 6.4 Hz, C≡$NC_6H_4OCH_2CH_2$), 6.93 (d, 2H, J = 9.2 Hz, C≡NC_6H_4O−), 7.06 (d, 2H, J = 8.3 Hz, C≡CC_6H_4), 7.39 (d, 2H, J = 8.3 Hz, C≡CC_6H_4), 7.45 (d, 2H, J = 9.2 Hz, C≡NC_6H_4O−). IR ν(C≡N)/cm^{-1}: 2218 (KBr), 2214 (CH_2Cl_2). Analysis calculated for $C_{37}H_{54}NOAu$ (%): C, 61.23; H, 7.49; N, 1.93. Found: C, 61.18; H, 7.22; N, 2.00.

***m* = 14, *n* = 8.** Yield: 89%. ^{1}H RMN ($CDCl_3$, 300 MHz): δ, 0.89 (m, 6H, CH_3), 1.26−1.81 (m, 36H, alkyl chain), 2.57 (t, 2H, J = 7.0 Hz, C≡$CC_6H_4CH_2$), 3.99 (t, 2H, J = 6.6 Hz, C≡$NC_6H_4OCH_2$), 6.93 (d, 2H, J = 9.2 Hz, C≡NC_6H_4O−), 7.06 (d, 2H, J = 7.9 Hz, C≡CC_6H_4), 7.39 (d, 2H, J = 7.9 Hz, C≡CC_6H_4), 7.44 (d, 2H, J = 9.2 Hz, C≡NC_6H_4O−). IR ν(C≡N)/cm^{-1}: 2213 (KBr), 2214 (CH_2Cl_2). Analysis calculated for $C_{37}H_{54}NOAu$ (%): C, 61.23; H, 7.50; N, 1.93. Found: C, 61.23; H, 7.18; N, 1.84.

***m* = 14, *n* = 14.** Yield: 91%. ^{1}H RMN (δ, $CDCl_3$, 300 MHz): 0.89 (m, 6H, CH_3), 1.26−1.80 (m, 48H, alkyl chain), 2.57 (t, 2H, J = 7.5 Hz, C≡$CC_6H_4CH_2$), 3.98 (t, 2H, J = 6.6 Hz, C≡$NC_6H_4OCH_2$), 6.93 (d, 2H, J = 8.8 Hz, C≡NC_6H_4O−), 7.06 (d, 2H, J = 7.9 Hz, C≡CC_6H_4), 7.39 (d, 2H, J = 7.9 Hz, C≡CC_6H_4), 7.44 (d, 2H, J = 8.8 Hz, C≡NC_6H_4O−). IR ν(C≡N)/cm^{-1}: 2220 (KBr), 2214 (CH_2Cl_2). Analysis calculated for $C_{43}H_{66}NOAu$ (%): C, 63.76; H, 8.21; N, 1.73. Found: C, 63.51; H, 7.99; N, 2.01.

Synthesis of Au NP. Gold nanoparticles were prepared by decomposition of [Au(C≡C−C_6H_4−C_mH_{2m+1})(C≡N−C_6H_4−O−C_nH_{2n+1})] complexes. A typical procedure is as follows: 0.072 mmol of the corresponding gold complex was dissolved in 6 mL of toluene in a 25 mL flask connected to a condenser. The flask was placed in a previously thermostatted oil bath at 110 °C, under aerobic conditions for 2 or 14 h. The solvent was removed under vacuum conditions, and the residue extracted with hexane, which was evaporated to obtain the product as a brown solid.

For the decomposition in the liquid crystal state, [Au(C≡C−C_6H_4−$C_{14}H_{29}$)(C≡N−C_6H_4−O−C_2H_5)] (0.072 mmol) was heated in an open vial in the air for 14 h at 155 °C. At this temperature, the compound displays a SmA mesophase.

Synthesis of $H_{29}C_{14}C_6H_4CC$≡C−C≡$CC_6H_4C_{14}H_{29}$. This compound was prepared as reported for similar 1,3-diines.[47] To a solution of CuCl (7 mg, 0.07 mmol) and TMEDA (19 μL, 0.21 mmol) in 10 mL of acetone was added 4-tetradecylphenylacetylene (0.1 g, 0,34 mmol). Oxygen was bubbled in the solution for 2 h, giving rise the desired product as a white solid that was filtered and washed with acetone (3 × 10 mL). Yield: 46 mg, 46%. IR ν(C≡C)/cm^{-1}: 2140 (KBr). ^{1}H NMR (δ, $CDCl_3$, 300 MHz): 0.88 (m, 6H, CH_3), 1.25 (m, 44H, CH_2), 1.59 (m, 4H, C≡$CC_6H_4CH_2CH_2$), 2.60 (t, 4H, C≡$CC_6H_4CH_2$), 7.14 (d, 4H, H-aryl), 7.43 (d, 4H, H-aryl). DSC/°C (kJmol^{-1}): C−C′ 12 (13.9); C′-SmC 59 (29); SmC-SmA 70 (microscopic data); SmA−N-I 73 (16.9, combined enthalpies).

AUTHOR INFORMATION

Corresponding Author

*E-mail: scoco@qi.uva.es (S.C.); espinet@qi.uva.es (P.E.).

ACKNOWLEDGMENT

This work was sponsored by the DGI (Project CTQ2008-03954/BQU and INTECAT Consolider Ingenio-2010 CSD2006-0003) and the Junta de Castilla y León (Projects VA248A11-2 and VA281A11-2). R.C. and E.C. gratefully acknowledge financial support from the Spanish Ministerio de Ciencia e Innovación.

REFERENCES

(1) (a) Schmid, G. *Chem. Rev.* **1992**, *92*, 1709–1727. (b) Murray, R. W. *Chem. Rev.* **2008**, *108*, 2688–2720. (c) Daniel, M. C.; Astruc, D. *Chem. Rev.* **2004**, *104*, 293–346.

(2) Burda, C.; Chen, X.; Narayanan, R.; El-Sayed, M. A. *Chem. Rev.* **2005**, *105*, 1025–1102.
(3) (a) Chen, W.; Chen, S. W.; Ding, F. Z.; Wang, H. B.; Brown, L. E.; Konopelski, J. P. *J. Am. Chem. Soc.* **2008**, *130*, 12156–12162. (b) Andres, R. P.; Bein, T.; Dorogi, M.; Feng, S.; Henderson, J. I.; Kubiak, C. P.; Mahoney, W.; Osifchin, R. G.; Reifenberger, R. *Science* **1996**, *272*, 1323–1325. (c) Chen, S. W.; Ingram, R. S.; Hostetler, M. J.; Pietron, J. J.; Murray, R. W.; Schaaff, T. G.; Khoury, J. T.; Alvarez, M. M.; Whetten, R. L. *Science* **1998**, *280*, 2098–2101. (d) Berven, C. A.; Clarke, L.; Mooster, J. L.; Wybourne, M. N.; Hutchison, J. E. *Adv. Mater.* **2001**, *13*, 109–113. (e) Kamat, P. V. *J. Phys. Chem. B* **2002**, *106*, 7729–7744.
(4) (a) Sun, S. H.; Murray, C. B.; Weller, D.; Folks, L.; Moser, A. *Science* **2000**, *287*, 1989–1992. (b) Sun, T.; Seff, K. *Chem. Rev.* **1994**, *94*, 857–870.
(5) (a) Mallik, K.; Witcomb, M. J.; Scurrell, M. S. *Appl. Phys. A: Mater. Sci. Process.* **2005**, *80*, 797–801. (b) Zaera, F. *J. Phys. Lett.* **2010**, *1*, 621. (c) Li, Y.; Somorjal, G. A. *Nano Lett.* **2010**, *10*, 2289.
(6) (a) Lewis, L. N. *Chem. Rev.* **1993**, *93*, 2693–2730. (b) Bradley, J. S. In *Clusters and Colloids, From Theory to Applications*; Schmid, G., Ed.; VCH: Weinheim, Germany, 1994; pp 523−536. (c) Edwards, P. P.; Johnston, R. L.; Rao, C. N. R. In *Metal Clusters in Chemistry*; Braunstein, P., Oro, L. A., Raithby, P. R., Eds.; Wiley-VCH: Weinheim, Germany, 1998. (d) *Nanoparticles and Nanostructured Films, Preparation, Characterization and Applications*; Fendler, J. H., Ed.; Wiley-VCH: Weinheim, Germany, 1998. (e) Aiken, J. D.; Finke, R. G. *J. Mol. Catal. A* **1999**, *145*, 1–44. (f) Rao, C. N. R.; Kulkarni, G. U.; Thomas, P. J.; Edwards, P. P. *Chem. Soc. Rev.* **2000**, *29*, 27–35.
(7) Dellinger, T. M.; Braun, P. V. *Chem. Mater.* **2004**, *16*, 2201–2207.
(8) (a) Ontko, A. C.; Angelici, R. J. *Langmuir* **1998**, *14*, 1684–1691. (b) Horinouchi, S.; Yamanoi, Y.; Yonezawa, T.; Mouri, T.; Nishihara, H. *Langmuir* **2006**, *22*, 1880–1884. (c) Swanson, S. A.; McClain, R.; Lovejoy, K. S.; Alamdari, N. B.; Hamilton, J. S.; Scott, J. C. *Langmuir* **2005**, *21*, 5034–5039. (d) Kim, H. S.; Lee, S. J.; Kim, N. H.; Yoon, J. K.; Park, H. K.; Kim, K. *Langmuir* **2003**, *19*, 6701–6710. (e) Horswell, S. L.; O'Neil, I. A.; Schiffrin, D. J. *J. Phys. Chem. B* **2001**, *105*, 941–947. (f) Henderson, J. I.; Feng, S.; Bein, T.; Kubiak, C. P. *Langmuir* **2000**, *16*, 6183–6187.
(9) Stewart, M. P.; Maya, F.; Kosynkin, D. V.; Dirk, S. M.; Stapleton, J. J.; McGuiness, C. L.; Allara, D. L.; Tour, J. M. *J. Am. Chem. Soc.* **2004**, *126*, 370–378.
(10) Dirk, S. M.; Pylypenko, S.; Howell, S. W.; Fulghum, J. E.; Wheeler, D. R. *Langmuir* **2005**, *21*, 10899–10901.
(11) Ciszek, J. W.; Keane, Z. K.; Cheng, L.; Stewart, M. P.; Yu, L. H.; Natelson, D.; Tour, J. M. *J. Am. Chem. Soc.* **2006**, *128*, 3179–3189.
(12) (a) Patterson, M. L.; Weaver, M. J. *J. Phys. Chem.* **1985**, *89*, 5046–5051. (c) Feilchenfeld, H.; Weaver, M. J. *J. Phys. Chem.* **1989**, *93*, 4216–4282. (d) Zhang, S.; Chandra, K. L.; Gorman, C. B. *J. Am. Chem. Soc.* **2007**, *129*, 4876–4877.
(13) (a) *Metallomesogens*; Serrano, J. L., Ed.; VCH: Weinheim, Germany, 1996. (b) Donnio, B.; Guillon, D.; Bruce, D. W.; Deschenaux, R. *Metallomesogens, Comprehensive Organometallic Chemistry III: From Fundamentals to Applications*; Crabtree, R. H., Mingos, D. M. P., Eds.; Elsevier: Oxford, U.K.; Vol. 12, 2006; *Applications III: Functional Materials, Environmental and Biological Applications*; O'Hare, D., Ed.; Elsevier: Oxford, U.K.; ch. 12.05, pp 195−294.
(14) Alejos, P.; Coco, S.; Espinet, P. *New J. Chem.* **1995**, *19*, 799–805.
(15) Espinet, P. *Gold Bull.* **1999**, *32*, 127–134.
(16) Ferrer, M.; Mounir, M.; Rodríguez, L.; Rossell, O.; Coco, S.; Gómez-Sal, P.; Martín, A. *J. Organomet. Chem.* **2005**, *690*, 2200–2208.
(17) Kaharu, T.; Ishii, R.; Adachi, T.; Yoshida, T.; Takahashi, S. *J. Mater. Chem.* **1995**, *5*, 687–692.
(18) Xiao, H.; Cheung, K.-K.; Che, C.-M. *J. Chem. Soc., Dalton Trans.* **1996**, 3699–3703.
(19) Irwin, J.; Vittal, J. J.; Puddephatt, R. J. *Organometallics* **1997**, 3541–3547.
(20) Vicente, J.; Chicote, M.-T.; Abrisqueta, M.-D.; Jones, P. G. *Organometallics* **1997**, *16*, 5628–5636.
(21) Siemeling, U.; Rother, D.; Bruhn, C. *Organometallics* **2008**, *27*, 6419–6426.
(22) Puddephatt, R. J.; Treurnicht, I. *J. Organomet. Chem.* **1987**, *319*, 129–137.
(23) Castillejos, E.; Chico, R.; Bacsa, R.; Coco, S.; Espinet, P.; Pérez-Cadenas, M.; Guerrero-Ruiz, A.; Rodríguez-Ramos, I.; Serp, P. *Eur. J. Inorg. Chem.* **2010**, 5096–5102.
(24) (a) Sau, T. K.; Murphy, C. J. *J. Am. Chem. Soc.* **2004**, *126*, 8648–8649. (b) Shukla, S.; Priscilla, A.; Banerjee, M.; Bhonde, R. R.; Ghatak, J.; Satyam, P. V.; Sastry, M. *Chem. Mater.* **2005**, *17*, 5000–5005. (c) Wu, H. Y.; Chu, H. C.; Kuo, T. J.; Kuo, C. L.; Huang, M. H. *Chem. Mater.* **2005**, *17*, 6447–6451.
(25) (a) Sakai, T.; Alexandridis, P. *J. Phys. Chem. B* **2005**, *109*, 7766–7777. (b) J. Kimling, J.; Maier, M.; Ovenke, B.; Kotaidis, V.; Ballot, H.; Plech, A. *J. Phys. Chem. B* **2006**, *110*, 15700–15707. (c) Pong, B. K.; Elim, H. I.; Chong, J. X.; Trout, B. L.; Lee, J. Y. *J. Phys. Chem. C* **2007**, *111*, 6281–6287. (d) Ji, X. H.; Song, X. N.; Li, J.; Bai, Y. B.; Yang, W. S.; Peng, X. G. *J. Am. Chem. Soc.* **2007**, *129*, 13939–13948.
(26) Pileni, M. P. Metal Particles Made in Various Colloidal Self-Assemblies: Syntheses and Properties. In *Fine Particles: Synthesis, Characterization, and Mechanisms of Growth*; Sugimoto, T., Ed.; Marcel Dekker: New York, 2000.
(27) Polte, J.; Ahner, T. T.; Delissen, F.; Sokolov, S.; Emmerling, F.; Thünemann, A. F.; Kraehnert, R. *J. Am. Chem. Soc.* **2010**, *132*, 1296–1301.
(28) Shevchenko, E. V; Talapin, D. V.; Schnablegger, H.; Kornowski, A.; Festin, Ö.; Svelindh, P.; Haase, M.; Weller, H. *J. Am. Chem. Soc.* **2003**, *125*, 9090–9101.
(29) Alloyeau, D.; Prévot, G.; Le Bouar, Y.; Oikawa, T.; Langlois, C.; Loiseau, A.; Ricilleau, C. *Phys. Rev. Lett.* **2010**, *105*, 255901–255904.
(30) Wegner, H. A. *Chimia* **2009**, *63*, 44–48.
(31) Cui, L.; Zhang, G.; Zhang, L. *Bioorg. Med. Chem. Lett.* **2009**, *19*, 3884–3887.
(32) Brenzovich, W. E., Jr; Brazeau, J.-F.; Toste, F. D. *Org. Lett.* **2010**, *12*, 4728–4731.
(33) Kar, A.; Mangu, N.; Kaiser, H. M.; Beller, M.; Tse, M. K. *Chem. Commun.* **2008**, 386–388.
(34) Shao, Z.; Peng, F. *Angew. Chem., Int. Ed. Engl.* **2010**, *49*, 9566–8.
(35) Kim, S.; Ihm, K.; Kang, T.-H.; Hwang, S.; Joo, S.-W. *Surf. Interface Anal.* **2005**, *37*, 294–299.
(36) 1,4-Diphenylbutadiyne $C_6H_5-C\equiv C-C\equiv C-C_6H_5$ displays two IR bands in solution associated with the triple bonds: 2145 cm^{-1} (strong), A_g mode; 2216 cm^{-1} (medium), B_u mode. See: Nyquist, R. A.; Putzig, C. L. *Vib. Spectrosc.* **1992**, *4*, 35–38.
(37) Zhang, S.; Chandra, K. L.; Gorman, C. B. *J. Am. Chem. Soc.* **2007**, *129*, 4876–4877.
(38) Markovich, N.; Volinsky, R.; Jelinek, R. *J. Am. Chem. Soc.* **2009**, *131*, 2430–2431.
(39) Segura, Y.; López, N.; Pérez-Ramírez, J. *J. Catal.* **2007**, *247*, 383–386.
(40) Angelici, R. J.; Lazar, M. *Inorg. Chem.* **2008**, *47*, 9155–9165.
(41) Coates, G. E.; Parkin, C. *J. Chem. Soc.* **1962**, 3220–3226.
(42) Mingos, D. M. P.; Yau, J.; Menzer, S.; Williams, D. J. *Angew. Chem., Int. Ed. Engl.* **1995**, *34*, 1894–1895.
(43) Kilpin, K. J.; Horvath, R.; Jameson, G. B.; Telfer, S. G.; Gordon, K. C.; Crowley, J. D. *Organometallics* **2010**, 6186–6195.
(44) Elchenbroich, C.; Salzer, A. *Organometallics*, 2nd ed.; VCH: Weinheim, Germany, 1992. ISBN: 3-527-28164-9.
(45) Berenguer, J. R.; Lalinde, E.; Moreno, M. T. *Coord. Chem. Rev.* **2010**, *254*, 832–875.
(46) Praefcke, K.; Khone, B.; Guthier, K.; Johnen, N.; Singer, D. *Liq. Cryst.* **1989**, *5*, 233–249.
(47) Hay, A. S. *J. Org. Chem.* **1962**, *27*, 3320–3321.